



Published in final edited form as:

*Dev Biol.* 2010 August 15; 344(2): 968–978. doi:10.1016/j.ydbio.2010.06.019.

## Morphogenesis of the Developing Mammary Gland: Stage-Dependent Impact of Adipocytes

Shira Landskroner-Eiger<sup>1</sup>, Jiyoung Park<sup>2</sup>, Davelene Israel<sup>3</sup>, Jeffrey W. Pollard<sup>4</sup>, and Philipp E. Scherer<sup>2,\*\*</sup>

<sup>1</sup>Department of Cell Biology, Albert Einstein College of Medicine, 1300 Morris Park Avenue, Bronx, NY 10461

<sup>2</sup>Touchstone Diabetes Center, Departments of Internal Medicine & Cell Biology, University of Texas Southwestern Medical Center, Dallas, Texas, 75390-8549

<sup>3</sup>Department of Medicine, Diabetes Research Center, Albert Einstein College of Medicine, Bronx, NY 10461

<sup>4</sup>Departments of Developmental and Molecular Biology, Center of Reproductive Biology and Womens' Health, Albert Einstein Cancer Center, Albert Einstein College of Medicine, Bronx, NY 10461

### Abstract

Mammary gland development is critically dependent on the interactions between the stromal and the epithelial compartments within the gland. These events are under the control of a complex interplay of circulating and locally-acting hormones and growth factors. To analyze the temporal and quantitative contributions of stromal adipocytes, we took advantage of the FAT-ATTAC mice ("Apoptosis Through Triggered Activation of Caspase-8"), a model of inducible and reversible loss of adipocytes. This loss can be achieved through the induced dimerization of a caspase-8 fusion protein. In the context of female mice, we can achieve ablation of mammary adipocytes relatively selectively without affecting other fat pads. Under these conditions, we find that adipocytes are essential for the formation of the extended network of ducts in the mammary gland during puberty. Beyond their role in development, adipocytes are also essential to maintain the normal alveolar structures that develop during adulthood. Loss of adipose tissue initiated 2 weeks after birth triggers fewer duct branching points, fewer terminal end buds (TEBs), and also triggers changes in proliferation and apoptosis in the epithelium associated with the TEBs. The reduced developmental pace that adipocyte-ablated glands undergo is reversible, as the emergence of new local adipocytes, upon cessation of treatment, enables the ductal epithelium to resume growth. Conversely, loss of local adipocytes initiated at 7 weeks of age resulted in excessive lobulation, indicating that adipocytes are critically involved in maintaining proper architecture and functionality of the mammary epithelium. Collectively, using a unique model of inducible and reversible loss of adipocytes, our observations suggest that adipocytes are required for proper development during puberty and for the maintenance of the ductal architecture in the adult mammary gland.

---

© 2010 Elsevier Inc. All rights reserved.

\*\*Corresponding author. Tel: (214) 648-8715; Fax: (214) 648-8720; philipp.scherer@utsouthwestern.edu.

**Publisher's Disclaimer:** This is a PDF file of an unedited manuscript that has been accepted for publication. As a service to our customers we are providing this early version of the manuscript. The manuscript will undergo copyediting, typesetting, and review of the resulting proof before it is published in its final citable form. Please note that during the production process errors may be discovered which could affect the content, and all legal disclaimers that apply to the journal pertain.

## Keywords

Mammary Gland; Stroma; Adipocytes

---

## Introduction

The relevance of stromal contributions towards the growth of ductal epithelium in the mammary gland is widely appreciated and thought to be important for the development of the mammary architecture both during embryogenesis as well as in the postnatal phase. These stromal-derived factors and structural effects relate to a profound impact on ductal morphogenesis and elongation, stimulation of end bud growth and branching, and casein and lipid accumulation within the epithelium (Hinck and Silberstein, 2005; Howlett and Bissell, 1993; Wiseman and Werb, 2002). Co-transplantation studies show that the embryonic mammary epithelium can form salivary gland-like structures if it is combined with salivary gland mesenchyme and then grafted under the renal capsule of a host mouse (Sakakura et al., 1976). The stromal environment in the mammary gland is rather complex and made up of many different cell types. These include cells such as adipocytes, fibroblasts, endothelial cells and various cells of the immune system (Darcy et al., 2000; Neville et al., 1998; Wiseman and Werb, 2002). Insights into the individual contributions of these cells are rather limited. Nevertheless, some efforts have been made to dissect the role of the different stromal cell populations in mammary development. For instance, the localization of macrophages around the terminal end buds of the mammary gland is critical for the formation of elongated ducts, branching and orientation of the ducts (Gouon-Evans et al., 2000; Van Nguyen and Pollard, 2002). It has also been suggested that brown adipocytes negatively regulate the degree of branching complexity and epithelial differentiation of the mammary gland in a systemic manner (Gouon-Evans and Pollard, 2002).

Adipocytes are highly abundant in the stroma of the mammary gland. These mammary-associated adipocytes undergo massive remodeling during lactation and involution, including lipid depletion and appearance as long projections during the former and regaining of the lipid stores and their morphogenic state in the latter (Neville et al., 1998). It is also postulated that during involution some adipocytes might dedifferentiate into preadipocytes or actually undergo apoptosis (Neville et al., 1998). Beyond their function as a lipid source, the role of the adipocyte as a rich source of endocrine factors is widely appreciated (Halberg et al., 2008). Some of the relevant adipocyte-derived factors (generally referred to as “adipokines”) include leptin, adiponectin, hepatocyte growth factor (HGF), collagen VI, IL-6 and TNF $\alpha$  (Trujillo and Scherer, 2006). Altered plasma levels of these factors are seen with obesity and related metabolic disorders and these altered levels have also been associated with increased breast cancer risk (Trujillo and Scherer, 2006; Vona-Davis and Rose, 2007). Our previous work characterized a broad spectrum of effects of soluble secretory products from adipocytes on the proliferative, anti-apoptotic and pro-angiogenic behavior of breast cancer both *in vitro* and *in vivo* (Iyengar et al., 2003; Iyengar et al., 2005; Landskroner-Eiger et al., 2009). These broad effects on transformed cells hint at a possible contribution of adipokines on normal growth processes ongoing in the developing and mature mammary gland. *In vitro* studies demonstrate that mammary adipocytes enhance morphological and functional differentiation of mammary epithelial organoids via undefined secreted soluble factors (Howlett and Bissell, 1993; Zangani et al., 1999). Co-transplantation experiments of embryonic mammary epithelium with either embryonic fibroblastic mesenchyme or embryonic fat pads concluded that it was the fatty stroma that was necessary for the mammary epithelium to undergo its characteristic morphogenesis (Sakakura et al., 1982). In a separate set of observations, the congenital lack of functional leptin (such as in *ob/ob* mice) or lack of the leptin receptor (*db/db* mice) leads to a complete failure of the

ductal epithelium to develop (Hu et al., 2002). One of the first attempts at defining the role of adipocyte-derived factors in mammary gland development *in vivo* was performed in the A-ZIP/F-1 mouse model. These mice never develop white adipose tissue and are therefore considered to be lipotrophic (Couldrey et al., 2002; Moitra et al., 1998). Female mice have reduced fertility with rudimentary mammary anlagen, severely distended mammary ducts and almost no pups survive beyond weaning (Couldrey et al., 2002). These mice are also severely diabetic, have an enlarged fatty liver and die prematurely (Moitra et al., 1998). This model has contributed much to our understanding of adipocyte physiology. However, as a consequence of the severe phenotype with prolonged congenital lipodystrophy, leading to lipotoxicity, it is difficult to distinguish between acute and chronic effects in this model. Interestingly, brown adipocytes, known to have thermogenic actions, have also been implicated in postnatal prepubertal mammary gland development (Gouon-Evans and Pollard, 2002).

Our *in vivo* approach focuses on an inducible depletion of adipocytes using our previously described FAT-ATTAC mouse model (“*Fat Ablation Through Triggered Activation of Caspase-8*”) (Pajvani et al., 2005). In this model, apoptosis of adipocytes can be induced at any developmental stage by administration of a FK1012 analog leading to the forced dimerization of a membrane-bound FKBP-caspase 8 fusion protein uniquely expressed in adipose tissue. In our initial studies, we examined male mice with respect to their metabolic response to the acute loss of adipose tissue. In male mice, adipocyte ablation occurred systemically and allowed for the elimination of almost all fat pads, even in an *ob/ob* background, a strain suffering from a very high degree of adiposity due to a mutation in the leptin gene (Pajvani et al., 2005).

Adipose tissue physiology is quite different between genders in the mouse. Circulating levels of many cytokines differ, as well as adipokine levels such as adiponectin and leptin (markedly higher in female mice compared with male mice) (Shi et al., 2009; Trujillo and Scherer, 2006). Here, we examined for the first time the female FAT-ATTAC mice, since our previous analysis focused exclusively on male mice. We find that conditions that lead to widespread elimination of adipocytes in male mice have only a minimal impact on fat pads in females. However, we observed that the mammary fat pad is considerably more susceptible to caspase-induced apoptosis than any other fat pads in the female mouse. Therefore, this enabled us to selectively ablate the mammary fat pad to probe for the consequences of the acute lack of *locally* acting, paracrine adipocyte-derived factors on ductal morphogenesis during the postnatal phase of mammary development. We focused on two critical milestones in the mammary gland: **A) *Pre-puberty through puberty***: At this stage, rapid development of the rudimentary ductal epithelium takes place through the formation of branching trees invading into the fatty stroma, together with dynamic changes of differentiation, proliferation and cell death occurring at the terminal end buds (TEBs). **B) *During adulthood*** when tertiary side-branching takes place, marking the initial formation of alveolar buds (Lu et al., 2006). Our findings demonstrate that local mammary associated adipocytes play an important role during all stages, thus supporting the view that adipocytes are potent mediators in the proper development and maintenance of ductal morphogenesis.

## Materials and Methods

### Animals

All animal experimental protocols were approved by the Institute for Animal Studies of the Albert Einstein College of Medicine and by the Institutional Animal Care and Use Committee of University of Texas Southwestern Medical Center at Dallas. Experiments presented were performed on a mixed, littermate controlled C57/BL6 and FVB background. Heterozygous FAT-ATTAC mice were crossed to wildtype mice. Mammary development

was compared between littermates of dimerizer-treated wildtype and dimerizer-treated FAT-ATTAC females.

### **Injection Protocol for Fat Ablation**

Administration of AP21087 (Clackson et al., 1998) (Ariad Pharmaceuticals) daily by intraperitoneal injections at a dose of 0.4mg/gr of body weight. Both wildtype and FAT-ATTAC animals were injected starting at either 2-weeks or 7-weeks of age, as indicated.

### **Whole Mount Staining and Histology of Mammary Gland**

Inguinal mammary glands were excised and spread onto glass slides. For histology, tissue was fixed 24hrs in 10% normal buffered formalin (Fisher) and embedded in paraffin. 5mm sections were stained with H&E, 3 sections per mouse were examined in a blinded fashion. Whole mount staining was done in alum carmine as described in <http://mammary.nih.gov/> and imaged on a Stemi SV11 stereo dissection microscope.

### **Morphologic Analysis of Mammary Gland Development**

To determine ductal lengths, mammary gland whole mount preparations were analyzed as described (Gouon-Evans et al., 2000; Roarty and Serra, 2007) with slight modifications, by measuring the distance of the longest duct from the nipple to the leading edge of the TEBs (Fig. 2) or by measuring the distance of the longest duct from the lymph node to the leading edge of the TEBs (Table 1). TEBs were counted in the whole mammary gland. Lateral secondary branching was determined for 2–3 major ducts per mammary gland.

### **Immunohistochemistry Analysis**

Terminal deoxynucleotidyltransferase-mediated dUPT nick end labeling (TUNEL) staining was performed according to the manufacturer's protocol (Chemicon) and at least 10 fields were imaged per mouse for further analysis. Quantification was assessed for the percentage of positive epithelial cells per TEBs and structures resembling TEBs in some circumstances. For evaluation of proliferation, mice were injected with bromodeoxyuridine (Sigma) (BrdU; 30 mg/kg) i.p. 2hrs before sacrifice and inguinal mammary glands were fixed 2hrs in 4% paraformaldehyde at RT followed by 22hr incubation at 4°C. Sections were stained using the BrdU Immunohistochemistry System (Calbiochem). Sections were analyzed by scoring the percentage of positive epithelial cells per TEB and structures resembling TEBs in some circumstances. For macrophage staining, slides were incubated overnight with a rat anti-mouse F4/80 antibody (Caltag), and further incubated with biotinylated rabbit anti-rat (Vector Laboratories) for 1 hour at room temperature. For b-casein detection a rabbit polyclonal was used (Santa Cruz Biotechnology) as described previously (Sotgia et al., 2009). The following additional antibodies were used for characterization of the mammary gland development: rabbit polyclonal p63 (Abcam), rabbit polyclonal alpha-smooth muscle actin (Abcam), rabbit polyclonal cytokeratin 8 (Abcam), rabbit polyclonal keratin 14 (Covance), rabbit polyclonal and keratin 5 (Covance). Slides were developed using a peroxidase detection kit (Vector Laboratories) and counterstained with hematoxylin (Sigma-Aldrich). Collagen content was determined by staining formalin-fixed paraffin sections in picro-sirius red (Sigma-Aldrich). Sections were imaged using a Zeiss Axioskop Plus with the AxioCam MRc camera, and either the 10x/N.A 0.3 or the 40x/N.A 0.65 objective.

### **Adiponectin, Glucose and Estradiol Measurements**

Adiponectin was measured from tail blood, with a mouse adiponectin RIA kit (LINCO Research, St. Charles, MO). Glucose measurements were performed following a 2hr fasting period with Precision Xtra blood glucose test strips (MediSense- ABBOTT). Estradiol

measurements were done using the Ultrasensitive Estradiol RIA (Diagnostic Systems Laboratories).

### RNA Isolation and Analysis

Mice were sacrificed and tissue was immediately harvested and frozen in liquid nitrogen. RNA was isolated from frozen mammary gland tissue by using Qiagen RNeasy Lipid tissue kit following the manufacturer's protocol. cDNA was synthesized from 2.5mg RNA using Superscript III and oligo dT (Invitrogen). All PCR reactions were normalized to actin mRNA. Quantitative PCR, using Syber Green I master mix, was performed in the Roche Lightcycler® 480 with the following primer sets: Actin: Forward: 5' TACCACAGGCATTGTGATGG 3', Reverse: 5' TTTGATGTCACGCACGATTT 3'; FAT-ATTAC Transgene: Forward: 5' CACCACATGCCACTCTCGTCTT 3', Reverse: 5' GGTGCTCCTCTGAATCAGTCTC 3'. b- casein Forward: 5' GGC ACA GGT TGT TCA GGC TT 3', Reverse: 5' GAA TGT TGT GGA GTG GCA GG 3'.

### Statistical Analysis

The results are shown as means  $\pm$  SEM. Statistical analysis was performed by the Student t-test. Significance was accepted at  $p < 0.05$ .

## Results

### Characterization of the FAT-ATTAC Model in Female Mice

To address the role of the mammary stromal adipocytes in postnatal mammary gland development, we needed a model in which we could ablate adipocytes at various stages of postnatal development. While a number of lipodystrophic and lipoatrophic models have been described (Moitra et al., 1998; Ross et al., 1993), our previously characterized FAT-ATTAC mice remain a unique model in which adipocytes can be ablated at any point during the lifespan of a mouse. These FAT-ATTAC mice are therefore ideally suited to temporally dissect specific consequences of lack of adipocyte-derived factors with relatively high resolution.

However, a critical gap in our previous observations was that we had performed our analysis exclusively on male mice. We therefore started with an initial characterization of the effectiveness of the caspase-8 mediated apoptosis in female derived fat. Conditions used for the ablation of fat pads in males were ineffective in females, suggesting a higher inherent resistance to caspase-8 mediated cell death (data not shown). Exposure to the dimerizer at a dose twice as high as in males, starting at 2 weeks of age for a treatment period of either 2 weeks or 4 weeks, resulted in a gradual reduction and ultimately severe depletion of the mammary gland adipose tissue. Other fat depots examined displayed minimal signs of adipocyte apoptosis and ablation. As judged by measuring the weight of excised inguinal mammary glands, a 2 and 4-week treatment demonstrated a 2.2 and 2.8-fold reduction in mammary gland mass respectively (Fig. 1A). Untreated 6-week old FAT-ATTAC mice showed a slight reduction in mammary gland mass although this did not mount to any statistical significance (Fig. 1A). In addition, H&E staining of mammary glands derived from untreated 6-week old FAT-ATTAC mice showed comparable histology to the littermate wildtype control mice (Fig. 1B). No reduction of adipocyte mass was observed in other fat depots. On the contrary, a modest, yet significant increase in fat pad mass was observed following a 4-week treatment, as shown in the case of the gonadal depot (Fig. 1C). This has previously been reported for other models using partial lipectomy. Even in humans, local removal of subcutaneous fat through liposuction is associated with an increase in mass in other pads (Mauer et al., 2001). All these studies conclude that removal of fat in one particular fat pad resulted in a compensatory expansion of other fat pads. Under those

conditions, compensatory expansion of other fat pads occurs even in the absence of a concomitant increase in food intake (Mauer et al., 2001). Interestingly, the loss of mammary adipocytes did not have a significant impact on total body weight (data not shown). In contrast to our previous observations in fatless male FAT-ATTAC mice, a subtle yet significant increase in fasting glucose levels was observed in females upon fat ablation (Fig. 1D). Importantly, the differential response between the two adipose depots in our FAT-ATTAC females was not a result of variability in transgene mRNA expression, as judged by qRT-PCR measurements at baseline (Fig. 1E). These results highlight the differences in apoptotic susceptibility between the various fat depots in females. From the perspective of studying the development of the mammary gland, female FAT-ATTAC mice offer an ideal system in light of the near complete ablation of functional mammary fat while leaving other fat pads minimally affected. Therefore, we conclude that we have established conditions that allow us to severely deplete the mammary gland adipocytes rather specifically without concomitant loss of other pads.

### Ductal Morphogenesis of the FAT-ATTAC Mammary Gland During Puberty

We analyzed whole mounts isolated from inguinal mammary glands of these mice with treatment starting at 2-weeks of age for either 2 or 4-weeks. A clear inhibition of ductal outgrowth was observed at both time points upon removal of functional adipocytes from mammary glands (Fig. 2A, B). Given that ductal growth occurs at the terminal end buds (TEBs), we also noticed a 1.7-fold and 4.4-fold reduction in the number of TEBs in adipocyte-depleted glands compared to wildtype glands at both the short and longer treatment regimen respectively (Fig. 2C). Lastly, the absence of extensive ductal side branching and filling in of inter-ductal spaces, was also a prominent feature of the adipocyte-ablated mammary glands when compared to wildtype glands (Fig. 2D). Collectively, these observations highlight the critical role that adipocytes play in orchestrating the organization and morphology of the mammary ductal architecture after birth.

A histological examination confirmed the disruption of the adipose architecture and apoptosis of adipocytes residing in the mammary gland (Fig. 3A **panel a–c**). The severe depletion of mammary adipocytes resulted in an irregular shape of the ducts, with fewer duct branching points and fewer TEBs (Fig. 3A **panel a–c**). Similar to what has been reported in the A/ZIP-F-1 mouse model, ducts often contained eosinophilic material in the lumen (data not shown). Concomitant with the ablation of functional adipocytes, a net increase of infiltrating macrophages surrounding the apoptotic adipocytes was observed, as highlighted using the macrophage specific F4/80 antigen (Fig. 3B **panel a–b**) (Gouon-Evans et al., 2000; Pajvani et al., 2005). No obvious change in macrophage distribution was observed within the epithelium proper of the mammary gland or in its immediate proximal surroundings (Fig. 3B **panel c–d**), reflecting the highly specific nature of the cellular ablation that is restricted to adipocytes. In addition, as observed using Sirius Red staining for collagen content, massive remodeling of the extracellular matrix was seen throughout the mammary gland, most likely indicative of changes in fibrous collagen content as a result of the loss of functional adipocytes (Fig. 3C **panel a–b**). An overall increase in collagen content was observed using Masson's Trichrome staining depicting accumulation of collagen I and collagen III (blue stain) distributed around the mammary epithelium as well as around the apoptotic adipocytes (Fig. 3C **panel c–d**). These dramatic modifications in extracellular components may be critical for mammary gland morphogenesis, organization and development (Fata et al., 2004; Ghajar and Bissell, 2008).

To further characterize the ductal features of the mammary gland in the FAT-ATTAC mice, sections of animals treated for 4-weeks were analyzed by immunohistochemistry for a spectrum of both basal and luminal epithelial markers (Mikaelian et al., 2006). There was no

significant change in expression levels or localization of  $\alpha$ -smooth muscle actin, keratin 5, keratin 14 or p63 in the ducts examined and altogether a similar pattern was detected in both wild-type and FAT-ATTAC treated animals (Fig. 4 **panel a–h**). Interestingly, the luminal marker cytokeratin 8 demonstrated a heterogenic pattern in the FAT-ATTAC treated animals compared to wild-type, where some ducts in the adipocyte-free environment displayed a collapsed lumen filled with layers of cytokeratin 8 positive cell clusters (Fig. 4 **panel i–j**). This was observed with a much smaller frequency the wild-type animals. These cumulative alterations in ductal features may be due to the loss of the mechanical and physical support provided by the adipocytes. Yet, as suggested by others (Howlett and Bissell, 1993; Zangani et al., 1999), the role of adipocytes are likely to stretch beyond mechanical support and include soluble adipokines that modulate the ductal epithelium growth via paracrine interactions.

### **Histological Analysis Confirms a Differential Response Between the Mammary and the Gonadal Adipose Tissue**

Confirming our initial observations of a differential response between different fat depots, a 2-week treatment resulted in a modest response of the gonadal adipose tissue with minimal disruption of adipose structure (Fig. 5A **panel a–b**). This included marginal infiltration of macrophages into this depot as assessed via F4/80 staining (Fig. 5A **panel d–e**). By 4 weeks of treatment, a gradual increase in alteration of adipocyte histology was observed in the gonadal fat pads as a heterogeneous population of adipocytes was apparent (Fig. 5A **panel c**) with a slight increase in number of infiltrating macrophages (Fig. 5A **panel f**). Altogether, the apoptotic response of the mammary associated adipocytes was significantly accelerated compared to only a mild response in the gonadal fat pad.

### **Shifting the Balance of Apoptosis and Proliferation**

The inhibitory effects on the architecture of the mammary tree elicited in our inducible model could be the result of alterations in proliferation and/or apoptosis of the epithelial compartment. TEBs are highly mitotic epithelial structures that are found only during active outgrowth into the fat pad. We have focused our analysis on the TEBs of wild-type animals and structures resembling TEBs in FAT-ATTAC treated mice, as classical TEBs structures were difficult to observe histologically in the fatless mammary glands. BrdU incorporation revealed more than a 3-fold decrease in proliferation of epithelial cells within the TEBs of mammary glands derived from FAT-ATTAC mice compared to wild-type glands injected with the dimerizer (Fig. 6A). TUNEL staining indicated that mammary glands of FAT-ATTAC mice exhibited over a 2-fold decrease in apoptosis within the TEBs, which may be the underlying reason for the higher abundance of multi-layered ducts (Fig. 6B). Immunohistochemically, luminal cells in TEBs of wild-type animals are strongly positive for keratin 8. Mammary glands of FAT-ATTAC treated mice were also positive for cytokeratin 8, yet displayed a generally looser and less organized appearance of the cytokeratin 8 positive structures resembling TEBs (Fig. 6C). Together, these observations highlight the prominent role of adipocytes in ductal morphogenesis via shaping both proliferation and apoptosis of the TEBs, steps that are crucial for both the formation of the lumen and ductal growth.

### **Normalization of Mammary Gland Growth in the FAT-ATTAC Mouse After Restoration of Adipogenesis**

Another aspect highlighted by our original studies in FAT-ATTAC mice is the reversibility of the adipose tissue ablation. Upon stopping the injections with dimerizer, we observed a regeneration of the adipocytes in fat pads (Pajvani et al., 2005). We therefore wanted to take advantage of this phenomenon in the current studies as well. We treated mice starting at 2-weeks of age for a 2 week period, followed by a 2-week period during which injections of

the dimerizer was ceased. The regenerative 2 week recovery phase is insufficient to restore adipose tissue mass. At this point, excised mammary glands derived from FAT-ATTAC mice still weigh significantly less than WT derived mammary glands (Fig. 7A). However, following cessation of dimerizer treatment, extensive patches of emerging adipose tissue in FAT-ATTAC mammary glands can be observed with a dramatic reduction in collagen deposition. These emerging regions appear histologically identical to wildtype mice, indicating that in the absence of continued dimerizer treatment, endogenous pre-adipocytes can successfully differentiate, enabling gradual adipose tissue regeneration (Pajvani et al., 2005) (Fig. 7B). The loss of adipocytes can diagnostically be monitored by assessing plasma levels of adiponectin, an adipocyte-specific secretory protein that can be measured with high sensitivity. Loss of functional fat cells entails a dramatic drop in the circulating levels of adiponectin (Pajvani et al., 2005). Indeed, during the course of dimerizer treatment in female mice, circulating adiponectin levels dropped within the first 4 days of treatment (data not shown), and are maintained at low levels during the course of treatment demonstrating a 70–75% reduction compared to wildtype injected littermates (Fig. 7C). 2 weeks post cessation of the dimerizer treatment, circulating levels of adiponectin were partially restored in the FAT-ATTAC mice (Fig. 7C), indicating that adipocyte progenitor cells are intact and the effect of adipocyte apoptosis is reversible. These measurements of circulating adiponectin highlight the important contribution that mammary adipose tissue makes towards systemic adiponectin levels. We did not observe the marked >95% reduction of circulating adiponectin observed in male FAT-ATTAC mice (Pajvani et al., 2005), most likely because the robust ablation of adipose tissue in females is restricted to the mammary fat pad. Interestingly, whole-mount analysis of the mammary gland revealed an almost full reversal of the mamotrophic phenotype. Although the number of secondary branches were still significantly lower in FAT-ATTAC mammary glands compared to the wildtype littermates, we observed similar number of TEBs and the resumption of ductal extension in the FAT-ATTAC mice relative to wildtype treated littermates, thus demonstrating a significant recovery to the normal architecture (Fig. 7D, Table 1). Thus, despite a sustained lower mammary gland mass following the recovery phase, the emerging functional adipocytes are sufficient to yield a considerable recovery and normalization of mammary gland growth. These observations suggest that the development of the ductal epithelium is not obligatorily coupled to other developmental processes in a time-restricted manner, but can proceed at later stages as well. Collectively, this suggests that in the absence of functional adipocytes in the mammary stroma, critical factors are missing that are usually required for the normal development of an organized mammary gland.

### Ductal Morphogenesis of the FAT-ATTAC Mammary Gland During Adulthood

Mammary development may be separated into embryonic, pubertal and adult phases, each of which is differentially regulated. The adult tertiary side-branching requires progesterone and prolactin in addition to local bi-directional crosstalk between the developing ductal epithelium and stromal cells (Naylor and Ormandy, 2002; Sternlicht et al., 2006). We thus tested whether the local adipocyte milieu is responsible for shaping the adult tertiary side-branching pattern and whether it is also important for the maintenance of fully developed mammary epithelial structures. Mice were treated with dimerizer for a 3-week period starting at 7-weeks of age, a time when the mice have fully developed their ductal structures. Similar to previous treatments, mammary gland mass was sharply decreased in these experiments as well, an indication that adipocytes were severely depleted at that stage (data not shown). Whole mount analysis showed main ductal branches to be thicker in FAT-ATTAC mammary glands compared to wildtype-derived mammary glands. Interestingly, 60% of the FAT-ATTAC mice demonstrated ductal epithelium with a highly tertiary branching pattern that was significantly different from that of wildtype-derived mammary glands (Fig. 8A **panel a–b**). An additional 30% of the remaining FAT-ATTAC animals also



demonstrated tertiary branching, but to a lesser degree. Importantly, none of the wildtype-derived mammary glands displayed such appearance. In addition, H&E staining of sections revealed the FAT-ATTAC mammary glands contained closely packed regions of alveoli similar to early pregnancy (Fig. 8A **panel c–d**). We also detected that the FAT-ATTAC mammary glands contained curvilinear ducts often filled with eosinophilic material, as well as ducts with collapsed lumens. Notably, estradiol measurements at the endpoint showed a similar spectrum of estradiol levels ranging between <5pg/ml to 19pg/ml in both wild-type and the FAT-ATTAC mice (Fig. 8B), suggesting that local depletion of functional adipocytes does not have an impact on the systemic hormonal milieu.

To investigate the formation of the tertiary branching pattern, we examined this phenomenon further. The mechanical destabilization of the overall gland architecture caused by the rapid disappearance of most adipocytes is reminiscent of the type of reconfiguration of the mammary gland at the beginning of pregnancy and even more so at lactation. In other words, we wanted to examine whether the sudden disappearance of functional adipocytes could trigger alveolar differentiation. To test this, both mRNA and protein levels of the milk protein b-casein were measured. The mammary glands of FAT-ATTAC mice treated with dimerizer 7–10 weeks of age demonstrated a 5-fold increase of mRNA levels for  $\beta$ -casein compared to wild-type dimerized mice (Fig. 8C). In support of that, immunohistochemistry analysis of b-casein also indicated a marked increase at the protein level in FAT-ATTAC-dimerized mice with considerable amounts accumulating in the alveolar lumens (Fig. 8D). Thus, a spatial and temporal depletion of adipocytes in the mature gland triggers a premature lobuloalveolar development with expression of b-casein.

## Discussion

Given the composition of the mammary gland in which adipocytes are a major constituent by both volume and cell number, FAT-ATTAC mice offer a unique possibility for the temporal dissection of the contributions of adipocytes towards mammary gland development. This type of experiment could not be performed to date for lack of an appropriate model. We were able to successfully ablate functional adipocytes in the mammary gland with minimal impact on other depots. This highlights the distinct characteristics of each fat pad, similar to the situation seen in a number of lipodystrophies (such as a HIV-associated lipodystrophy) in which fat pads are differentially affected, and therefore display a distinct behavior in different anatomical sites (Carr et al., 1998). The different fat pads can be viewed as distinct mini-organs that have distinct properties with respect to metabolic activity and hormone production and signaling (Giorgino et al., 2005; Trujillo and Scherer, 2006).

We have demonstrated that a severe depletion of adipocytes in the mammary gland during puberty leads to mamotrophic ductal growth and to alterations of ductal morphogenesis. Specifically, we observed an inhibition of ductal outgrowth, secondary ductal growth and number of TEBs. In addition, mammary glands depleted of adipocytes show a decrease in apoptosis, resulting in an increased density of luminal cells, as suggested by the clustering of cytokeratin 8 positive cells in the lumen of mammary ducts. Appropriate timing of the apoptosis of inner body cells is a crucial step during the formation of the lumen (Fata et al., 2004). Moreover, we observed a decrease in proliferation in the outer layer cap cells of the TEBs, cells that are normally considered the central point of growth in the mammary epithelium (Rosen, 2004). We have demonstrated the reversibility of the growth inhibition, as a 2-week cessation of treatment allowed a significant regeneration of functional adipocytes, resulting in re-growth of the mammary gland. Nevertheless, despite the functional recovery of the adipocytes, mammary gland mass remains somewhat reduced, however the emerging functional adipocytes are sufficient to yield a considerable recovery

and normalization of mammary gland growth. Thus, the temporary elimination of mature adipocytes does not have an irreversible effect on the mammary gland nor its multipotent mammary stem cells that are required for outgrowth, even though the continued presence of adipocytes is clearly required to maintain the normal architecture of the gland.

Our observations are consistent with previous work done with the A-ZIP/F-1 transgenic mouse model, which congenitally lacks white adipose tissue throughout life. It was apparent in these studies that adipocytes play a vital role in mammary gland development (Couldrey et al., 2002; Moitra et al., 1998). In contrast to these observations, we show here that this is due to the depletion of the local mammary-associated adipocytes, rather than a systemic and prolonged depletion of adipose stores that the A-ZIP F-1 mice suffer from. The complete failure of adipose tissue to ever develop leads to profound systemic anomalies including abnormal liver function, diabetes and early death (Moitra et al., 1998). In our female FAT-ATTAC mice, no substantial secondary effects of mammary fat ablation on other tissues were observed. The robust impact on the mammary gland observed after 2 weeks of treatment with no dramatic histologic alterations in other depots examined, supports the idea that the reported changes in the ductal epithelial architecture are a direct consequence of the absence of local adipocyte-derived factors within the mammary gland rather than a systemic effect caused by the ablation of functional adipocytes in all fat pads. Moreover, it is well established that the overall expansion of the mammary epithelium is regulated by systemic hormones including estrogen, progesterone, glucocorticoids and prolactin in conjunction with local growth factors (Hinck and Silberstein, 2005). However, in the short term experiments, where mice were treated from 2 until 4-weeks of age, hormones such as estrogen are low as this precedes the time that the mice undergo a regular estrous cycle (Cohen et al., 2002), emphasizing that the local adipocyte-dependent milieu is likely the driving force for our observation. Even though we only see small systemic changes such as slightly elevated fasting glucose levels and a decrease in serum levels of adiponectin in FAT-ATTAC dimerized mice, we cannot rule out the possibility that the local depletion of mammary associated adipocytes may affect the mammary epithelium in both a paracrine fashion and via an endocrine loop.

A potential role of locally acting adipokines, such as leptin, adiponectin, hepatocyte growth factor (HGF) and additional factors has to be postulated. Evidence of leptin and adiponectin affecting mammary development has previously been demonstrated where genetically leptin-deficient and leptin receptor-deficient obese mice displayed profoundly impaired mammary gland morphogenesis (Hu et al., 2002), strongly arguing that leptin-signaling pathways are necessary for normal mammary gland development. As for adiponectin, our group has shown that adiponectin over-expressing mice reveal abnormal mammary development in which the ducts are underdeveloped, associated with reduced fertility (Combs et al., 2004; Kim et al., 2007; Landskroner-Eiger et al., 2009). Yet, given that restoration of leptin signaling in the brain is sufficient to reconstitute a normal ductal epithelial structure (*Park and Scherer, manuscript in preparation*) and that mice lacking adiponectin do not have a mamotrophic phenotype (Landskroner-Eiger et al., 2009), we believe that additional locally-acting adipokines such as HGF, may play a role in shaping the mammary gland architecture. We hypothesize that the absence of mammary associated adipocytes in the dimerizer-treated FAT-ATTAC model, causes a shift in the delicate balance between TGF $\beta$  and HGF levels, favoring a dominant inhibitory milieu enriched for TGF $\beta$  during puberty phase (Pollard, 2001).

Dimerizer treatment of FAT-ATTAC mice during adulthood resulted in the display of highly tertiary-branched ductal structures. Differences in side-branching patterns have previously been reported between different mouse strains (Naylor and Ormandy, 2002). However, given that all mice used in experiments are littermates, strain differences cannot

account for these differential side-branching patterns. In addition, although we made no effort to synchronize these mice with respect to their estrous cycle, the phenotypic differences were seen in the vast majority of the FAT-ATTAC mice examined, suggesting that this is independent of the estrous cycle. Our results indicate that depletion of adipocytes during adulthood induces a premature lobuloalveolar development. Similarly, in a type 1 diabetic model (the “PANIC-ATTAC mice”) that gradually loses lipids in mammary adipocytes due to the absence of the lipogenic actions of insulin, we observe a very similar tertiary branching pattern (*Park and Scherer, unpublished*). This is consistent with a model in which the displacement of adipocytes induces a premature lobuloalveolar development. It is yet to be determined whether dimerized FAT-ATTAC mice can indeed have functional lactating mammary glands.

The contribution of the adipocytes may not only relate to the paracrine supply of adipokines and chemokines, but they also contribute to the unique make up of the extracellular matrix within the mammary gland through the secretion of a large number of collagens and collagen – modifying enzymes (Halberg et al., 2008). We suggest that at multiple stages of postnatal mammary development, adipocytes provide not only the structural support, but they also set the hormonal milieu that actively regulates mammary morphogenesis by altering the local growth factor milieu as well as influencing the extracellular matrix composition. This extracellular matrix is a critical component in branching morphogenesis (Fata et al., 2004; Ghajar and Bissell, 2008; Lu et al., 2006). For example the site of fibronectin deposition has been correlated with branching pattern in the lung and kidney (Sakai et al., 2003). Thus, the temporal reciprocal epithelial-adipocyte signaling that drives the organization of the mammary ductal architecture has yet to be described. Given the dynamic adaptations that mammary-associated adipocytes undergo during normal mammary gland development, lactation and involution cycles, this model can greatly enhance our understanding in addressing the role of adipocytes in different stages of mammary gland development as well as in mammary tumorigenesis.

## Acknowledgments

We thank members of the Scherer and Pollard laboratories for assistance. We would like to thank the AECOM Diabetes Research and Training Center (DRTC) and Radioimmunoprecipitation Assay (RIA) Core Facility (Robin Sgueglia), the UT Southwestern Metabolic Core for phenotyping efforts. We further appreciate the expertise of Dr. Rani Sellers from the Histopathology Facility at AECOM. We thank Jiufeng Li and Jim Lee for technical assistance and Ariad Pharmaceuticals for providing the AP21087 dimerizer.

This work was supported by NIH grants R01-CA112023 (P.E.S.), R01-HD30820 (JWP), the Cancer Center from the National Cancer Institute P30-1330 (JWP), by Training Grant T32-GM04791 (Training Program in Cellular and Molecular Biology and Genetics) (SLE) and by a Department of Defense Post-Doctoral Award BC085909 (JP).

## References

- Carr A, Samaras K, Chisholm DJ, Cooper DA. Pathogenesis of HIV-1-protease inhibitor-associated peripheral lipodystrophy, hyperlipidaemia, and insulin resistance. *Lancet*. 1998; 351:1881–1883. [PubMed: 9652687]
- Clackson T, Yang W, Rozamus LW, Hatada M, Amara JF, Rollins CT, Stevenson LF, Magari SR, Wood SA, Courage NL, Lu X, Cerasoli F Jr, Gilman M, Holt DA. Redesigning an FKBP-ligand interface to generate chemical dimerizers with novel specificity. *Proc Natl Acad Sci U S A*. 1998; 95:10437–10442. [PubMed: 9724721]
- Cohen PE, Zhu L, Nishimura K, Pollard JW. Colony-stimulating factor 1 regulation of neuroendocrine pathways that control gonadal function in mice. *Endocrinology*. 2002; 143:1413–1422. [PubMed: 11897698]
- Combs TP, Pajvani UB, Berg AH, Lin Y, Jelicks LA, Laplante M, Nawrocki AR, Rajala MW, Parlow AF, Cheeseboro L, Ding YY, Russell RG, Lindemann D, Hartley A, Baker GR, Obici S, Deshaies

- Y, Ludgate M, Rossetti L, Scherer PE. A transgenic mouse with a deletion in the collagenous domain of adiponectin displays elevated circulating adiponectin and improved insulin sensitivity. *Endocrinology*. 2004; 145:367–383. Epub 2003 Oct 2023. [PubMed: 14576179]
- Couldrey C, Moitra J, Vinson C, Anver M, Nagashima K, Green J. Adipose tissue: a vital in vivo role in mammary gland development but not differentiation. *Dev Dyn*. 2002; 223:459–468. [PubMed: 11921335]
- Darcy KM, Zangani D, Shea-Eaton W, Shoemaker SF, Lee PP, Mead LH, Mudipalli A, Megan R, Ip MM. Mammary fibroblasts stimulate growth, alveolar morphogenesis, and functional differentiation of normal rat mammary epithelial cells. *In Vitro Cell Dev Biol Anim*. 2000; 36:578–592. [PubMed: 11212143]
- Fata JE, Werb Z, Bissell MJ. Regulation of mammary gland branching morphogenesis by the extracellular matrix and its remodeling enzymes. *Breast Cancer Res*. 2004; 6:1–11. [PubMed: 14680479]
- Ghajar CM, Bissell MJ. Extracellular matrix control of mammary gland morphogenesis and tumorigenesis: insights from imaging. *Histochem Cell Biol*. 2008; 130:1105–1118. [PubMed: 19009245]
- Giorgino F, Laviola L, Eriksson JW. Regional differences of insulin action in adipose tissue: insights from in vivo and in vitro studies. *Acta Physiol Scand*. 2005; 183:13–30. [PubMed: 15654917]
- Gouon-Evans V, Pollard JW. Unexpected deposition of brown fat in mammary gland during postnatal development. *Mol Endocrinol*. 2002; 16:2618–2627. [PubMed: 12403850]
- Gouon-Evans V, Rothenberg ME, Pollard JW. Postnatal mammary gland development requires macrophages and eosinophils. *Development*. 2000; 127:2269–2282. [PubMed: 10804170]
- Halberg N, Wernstedt-Asterholm I, Scherer PE. The Adipocyte as an Endocrine Cell. *Endocrinol Metab Clin North Am*. 2008; 37:753–768. [PubMed: 18775362]
- Hinck L, Silberstein GB. Key stages in mammary gland development: the mammary end bud as a motile organ. *Breast Cancer Res*. 2005; 7:245–251. Epub 2005 Oct 2003. [PubMed: 16280048]
- Howlett AR, Bissell MJ. The influence of tissue microenvironment (stroma and extracellular matrix) on the development and function of mammary epithelium. *Epithelial Cell Biol*. 1993; 2:79–89. [PubMed: 8353596]
- Hu X, Juneja SC, Maihle NJ, Cleary MP. Leptin--a growth factor in normal and malignant breast cells and for normal mammary gland development. *J Natl Cancer Inst*. 2002; 94:1704–1711. [PubMed: 12441326]
- Iyengar P, Combs TP, Shah SJ, Gouon-Evans V, Pollard JW, Albanese C, Flanagan L, Tenniswood MP, Guha C, Lisanti MP, Pestell RG, Scherer PE. Adipocyte-secreted factors synergistically promote mammary tumorigenesis through induction of anti-apoptotic transcriptional programs and proto-oncogene stabilization. *Oncogene*. 2003; 22:6408–6423. [PubMed: 14508521]
- Iyengar P, Espina V, Williams TW, Lin Y, Berry D, Jelicks LA, Lee H, Temple K, Graves R, Pollard J, Chopra N, Russell RG, Sasisekharan R, Trock BJ, Lippman M, Calvert VS, Petricoin EF 3rd, Liotta L, Dadachova E, Pestell RG, Lisanti MP, Bonaldo P, Scherer PE. Adipocyte-derived collagen VI affects early mammary tumor progression in vivo, demonstrating a critical interaction in the tumor/stroma microenvironment. *J Clin Invest*. 2005; 115:1163–1176. Epub 2005 Apr 1114. [PubMed: 15841211]
- Kim JY, van de Wall E, Laplante M, Azzara A, Trujillo ME, Hofmann SM, Schraw T, Durand JL, Li H, Li G, Jelicks LA, Mehler MF, Hui DY, Deshaies Y, Shulman GI, Schwartz GJ, Scherer PE. Obesity-associated improvements in metabolic profile through expansion of adipose tissue. *J Clin Invest*. 2007; 117:2621–2637. [PubMed: 17717599]
- Landskroner-Eiger S, Qian B, Muise ES, Nawrocki AR, Berger JP, Fine EJ, Koba W, Deng Y, Pollard JW, Scherer PE. Proangiogenic contribution of adiponectin toward mammary tumor growth in vivo. *Clin Cancer Res*. 2009; 15:3265–3276. [PubMed: 19447867]
- Lu P, Sternlicht MD, Werb Z. Comparative mechanisms of branching morphogenesis in diverse systems. *J Mammary Gland Biol Neoplasia*. 2006; 11:213–228. [PubMed: 17120154]
- Mauer MM, Harris RB, Bartness TJ. The regulation of total body fat: lessons learned from lipectomy studies. *Neurosci Biobehav Rev*. 2001; 25:15–28. [PubMed: 11166075]

- Mikaelian I, Hovick M, Silva KA, Burzenski LM, Shultz LD, Ackert-Bicknell CL, Cox GA, Sundberg JP. Expression of terminal differentiation proteins defines stages of mouse mammary gland development. *Vet Pathol.* 2006; 43:36–49. [PubMed: 16407485]
- Moitra J, Mason MM, Olive M, Krylov D, Gavrilova O, Marcus-Samuels B, Feigenbaum L, Lee E, Aoyama T, Eckhaus M, Reitman ML, Vinson C. Life without white fat: a transgenic mouse. *Genes Dev.* 1998; 12:3168–3181. [PubMed: 9784492]
- Naylor MJ, Ormandy CJ. Mouse strain-specific patterns of mammary epithelial ductal side branching are elicited by stromal factors. *Dev Dyn.* 2002; 225:100–105. [PubMed: 12203726]
- Neville MC, Medina D, Monks J, Hovey RC. The mammary fat pad. *J Mammary Gland Biol Neoplasia.* 1998; 3:109–116. [PubMed: 10819521]
- Pajvani UB, Trujillo ME, Combs TP, Iyengar P, Jelicks L, Roth KA, Kitsis RN, Scherer PE. Fat apoptosis through targeted activation of caspase 8: a new mouse model of inducible and reversible lipodystrophy. *Nat Med.* 2005; 11:797–803. Epub 2005 Jun 2019. [PubMed: 15965483]
- Pollard JW. Tumour-stromal interactions. Transforming growth factor-beta isoforms and hepatocyte growth factor/scatter factor in mammary gland ductal morphogenesis. *Breast Cancer Res.* 2001; 3:230–237. Epub 2001 Jun 2014. [PubMed: 11434874]
- Roarty K, Serra R. Wnt5a is required for proper mammary gland development and TGF-beta-mediated inhibition of ductal growth. *Development.* 2007; 134:3929–3939. [PubMed: 17898001]
- Rosen, J. Molecular mechanisms regulating breast development. In: Harris, JR.; L.M.; Morrow, M.; Osborne, CK., editors. *Diseases of the Breast.* Baltimore, MD: Lippincott, Williams and Wilkins; 2004. p. 15-26.
- Ross SR, Graves RA, Spiegelman BM. Targeted expression of a toxin gene to adipose tissue: transgenic mice resistant to obesity. *Genes Dev.* 1993; 7:1318–1324. [PubMed: 8330737]
- Sakai T, Larsen M, Yamada KM. Fibronectin requirement in branching morphogenesis. *Nature.* 2003; 423:876–881. [PubMed: 12815434]
- Sakakura T, Nishizuka Y, Dawe CJ. Mesenchyme-dependent morphogenesis and epithelium-specific cytodifferentiation in mouse mammary gland. *Science.* 1976; 194:1439–1441. [PubMed: 827022]
- Sakakura T, Sakagami Y, Nishizuka Y. Dual origin of mesenchymal tissues participating in mouse mammary gland embryogenesis. *Dev Biol.* 1982; 91:202–207. [PubMed: 7095258]
- Shi H, Seeley RJ, Clegg DJ. Sexual differences in the control of energy homeostasis. *Front Neuroendocrinol.* 2009
- Sotgia F, Casimiro MC, Bonuccelli G, Liu M, Whitaker-Menezes D, Er O, Daumer KM, Mercier I, Witkiewicz AK, Minetti C, Capozza F, Gormley M, Quong AA, Rui H, Frank PG, Milliman JN, Knudsen ES, Zhou J, Wang C, Pestell RG, Lisanti MP. Loss of caveolin-3 induces a lactogenic microenvironment that is protective against mammary tumor formation. *Am J Pathol.* 2009; 174:613–629. [PubMed: 19164602]
- Sternlicht MD, Kouros-Mehr H, Lu P, Werb Z. Hormonal and local control of mammary branching morphogenesis. *Differentiation.* 2006; 74:365–381. [PubMed: 16916375]
- Trujillo ME, Scherer PE. Adipose tissue-derived factors: impact on health and disease. *Endocr Rev.* 2006; 27:762–778. Epub 2006 Oct 2020. [PubMed: 17056740]
- Van Nguyen A, Pollard JW. Colony stimulating factor-1 is required to recruit macrophages into the mammary gland to facilitate mammary ductal outgrowth. *Dev Biol.* 2002; 247:11–25. [PubMed: 12074549]
- Vona-Davis L, Rose DP. Adipokines as endocrine, paracrine, and autocrine factors in breast cancer risk and progression. *Endocr Relat Cancer.* 2007; 14:189–206. [PubMed: 17639037]
- Wiseman BS, Werb Z. Stromal effects on mammary gland development and breast cancer. *Science.* 2002; 296:1046–1049. [PubMed: 12004111]
- Zangani D, Darcy KM, Shoemaker S, Ip MM. Adipocyte-epithelial interactions regulate the in vitro development of normal mammary epithelial cells. *Exp Cell Res.* 1999; 247:399–409. [PubMed: 10066368]

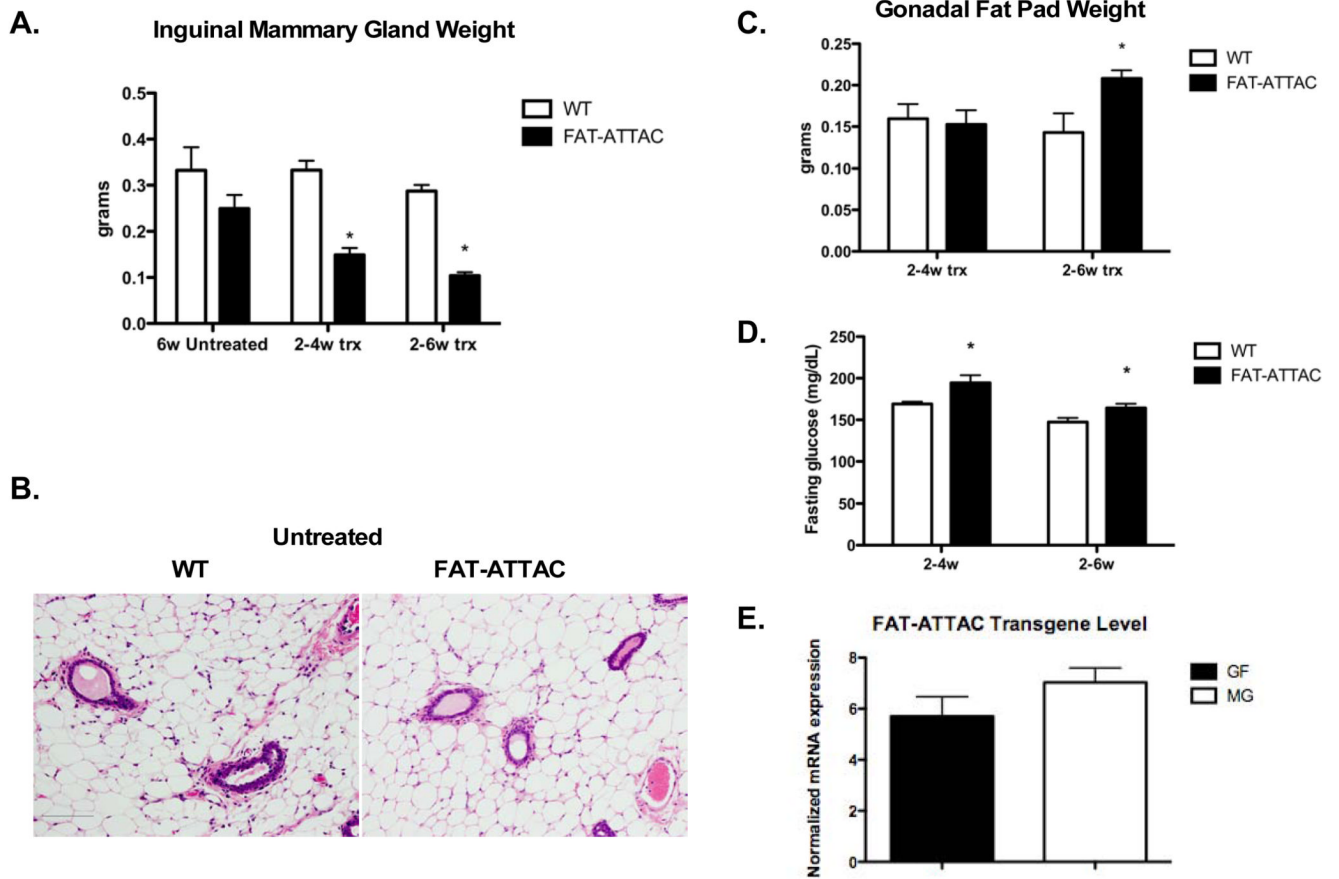


### Figure 1. Ablation of adipocytes following dimerizer treatment

Mice were injected with dimerizer starting at 2-weeks of age, for either 2 or 4 weeks. **A)** Excised inguinal mammary glands were weighed, demonstrating a 2.2 and 2.8-fold reduction in mammary gland mass following a 2 and 4-week treatment, respectively. (\* $p < 0.001$ ,  $n = 5-9$ /per group). **B)** H&E of the mammary gland of 6-week old untreated WT and FAT-ATTAC mice (Scale bar 100mm). **C)** Gonadal fat pads derived from same experiments as described, reveal an increase in mass following a 4-week dimerization protocol (\* $p < 0.05$ ,  $n = 6-10$ /per group). **D)** A modest, yet significant, increase in the fasting glucose levels of FAT-ATTAC mice was detected (\* $p < 0.05$ ,  $n = 5-13$ /per group). **E)** mRNA levels of the FAT-ATTAC transgene in the mammary gland (MG) and the gonadal fat pad (GF) was examined in untreated animals at 6-weeks of age. No significant difference was observed ( $n = 5$ /per group).

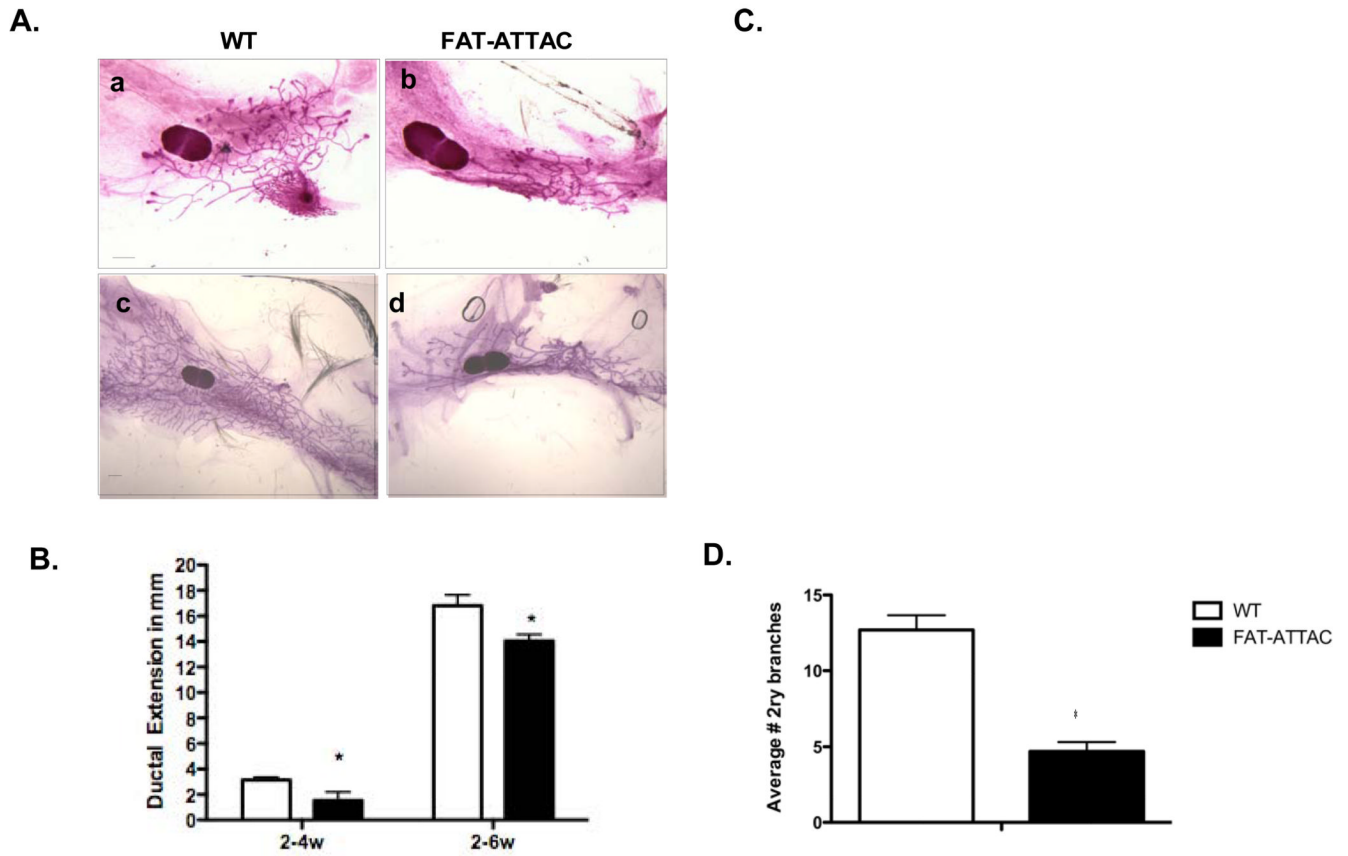


**Figure 2. Inhibition of ductal morphogenesis as a consequence of adipocyte depletion in the mammary stroma**

**A)** Representative whole mounts of inguinal mammary glands treated from 2-weeks of age for 2 weeks (panel a–b) or 4-weeks (panel c–d). (Scale bar 1mm). **B)** Quantification of ductal extension as measured for the longest duct. **C)** Quantification of the number of TEBs. (**B–C** \* $p < 0.05$ ,  $n = 5–13$ /per group). **D)** Average number of secondary branches per 0.5cm of major ducts in mice treated for 4-weeks with the dimerizer (\* $p < 0.05$ ,  $n = 4–5$ /per group).

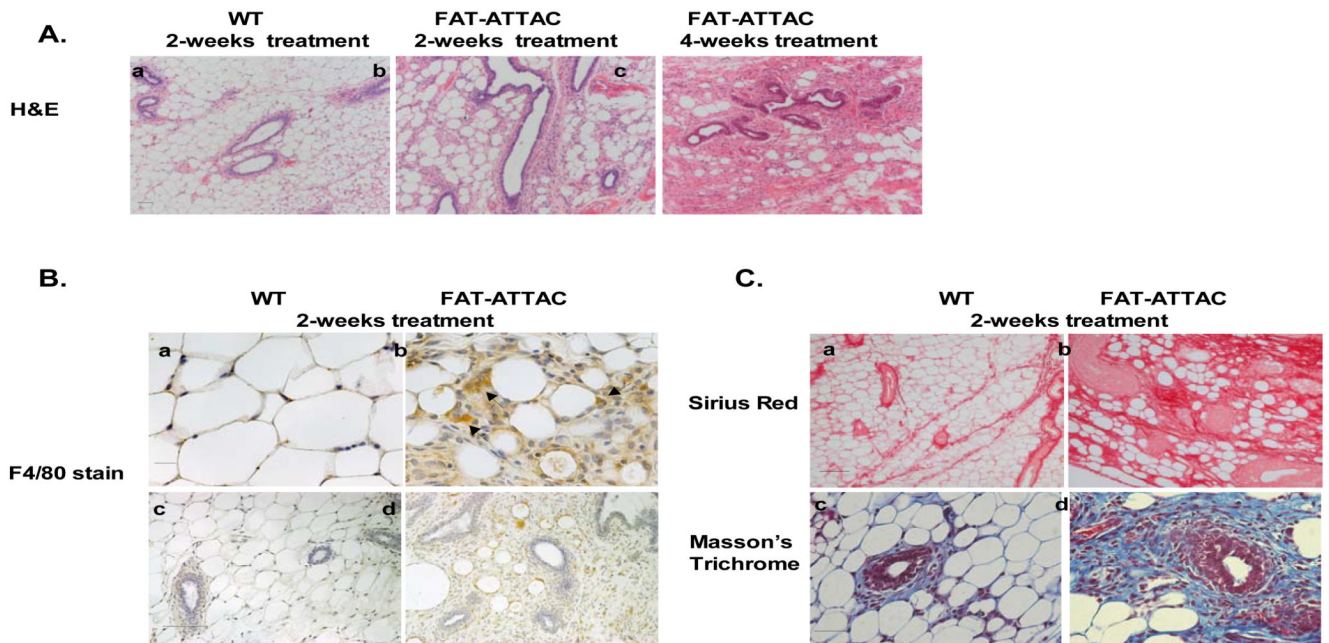


**Figure 3. Histological examination reveals an effective loss of adipocytes in the mammary adipose stroma resulting in abnormal ductal morphology**

Mice were subjected to treatment with the dimerizer from 2-weeks of age for a period of 2 or 4 weeks. **A)** H&E of the mammary gland (panel a–c) demonstrates that a 2-week treatment is sufficient to induce massive changes in the architecture of the adipocytes in the mammary stroma. These changes are exacerbated by 4-weeks of treatment. The ablation of mammary adipocytes resulted in irregular shape of the ducts. (Scale bar panel (a–c) 50mm, n=6–10/per group). **B)** Immunohistochemistry for macrophages using the F4/80 marker, as it is associated with local adipose structure disruption and apoptosis (Scale bar panel (a–b) 20mm, panel (c–d) 100mm). **C)** Sirius red staining (panel a–b) for collagen content at 4 weeks of age. Masson's Trichrome staining, at 4 weeks of age, highlighting primarily collagen I and collagen III (blue) demonstrating increase in collagen deposition throughout the mammary epithelium and stromal compartment (Scale bar panel (a–b) 100mm, panel (c–d) 50mm).



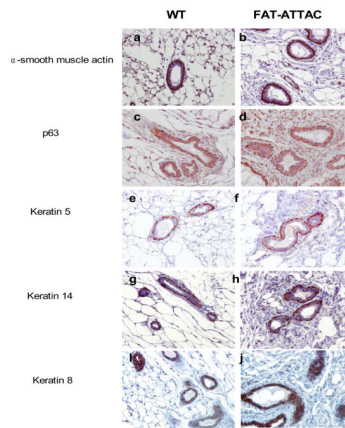


**Figure 4. Immunohistochemical characterization of mammary glands**

Mice were subjected to treatment with the dimerizer from 2-weeks of age for a period of 4 weeks. Immunohistochemical analysis for basal cells markers such as p63, α-smooth muscle, keratin 5 and keratin 14 did not reveal any apparent expression differences among treated wild-type and FAT-ATTAC mice. Cytokeratin 8 analysis of luminal cells revealed a higher degree of epithelial clustering with multiple layers of cells within the ducts (n=5/per group, Scale bar 50mm).

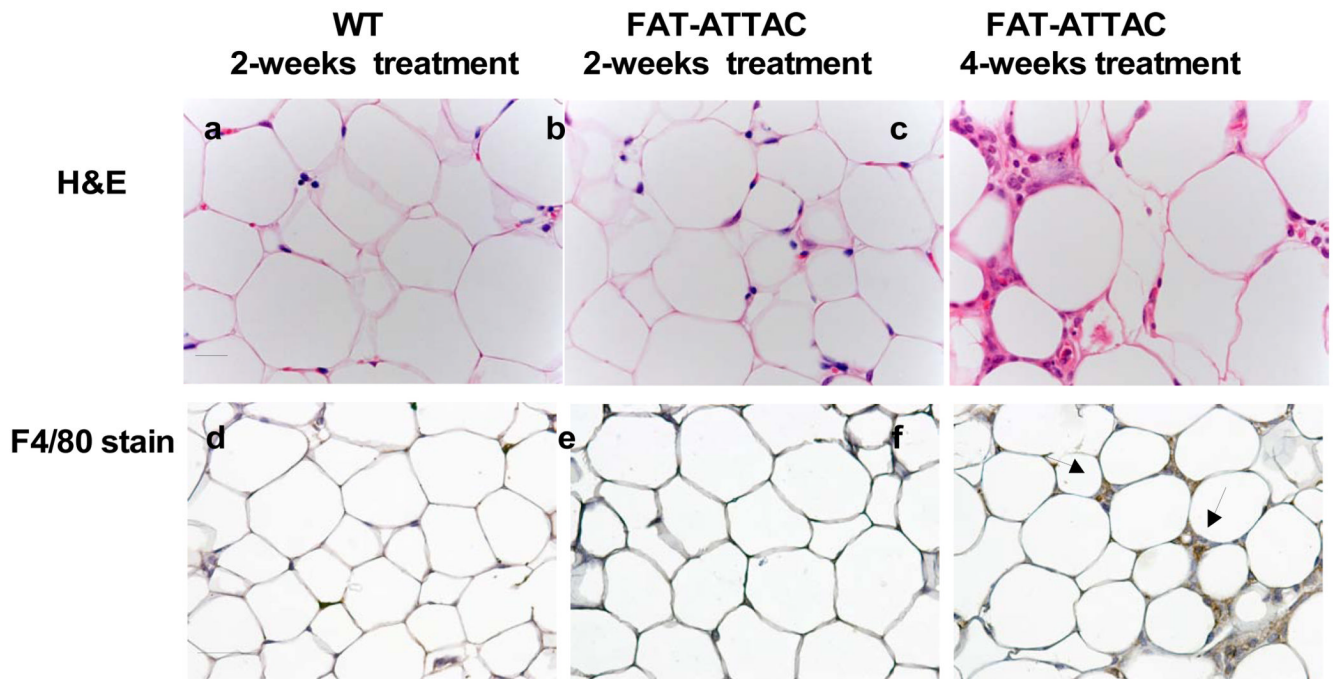


**Figure 5. Histological examination confirms a mild response in the gonadal fat pad**

Mice were subjected to treatment with the dimerizer from 2-weeks of age for a period of 2 or 4 weeks. As observed by H&E (panel a–c), the gonadal fat pad displays a subtle response to the dimerizer with minimal disruption of adipose structure following 2 weeks of treatment and a gradual increase in alteration of adipocyte histology following 4 weeks of treatment. Panel (d–f) display immunohistochemistry staining for macrophages using the F4/80 marker. (Scale bar panel (a–c) 20mm, panel (d–f) 50mm, n=6–10/per group).

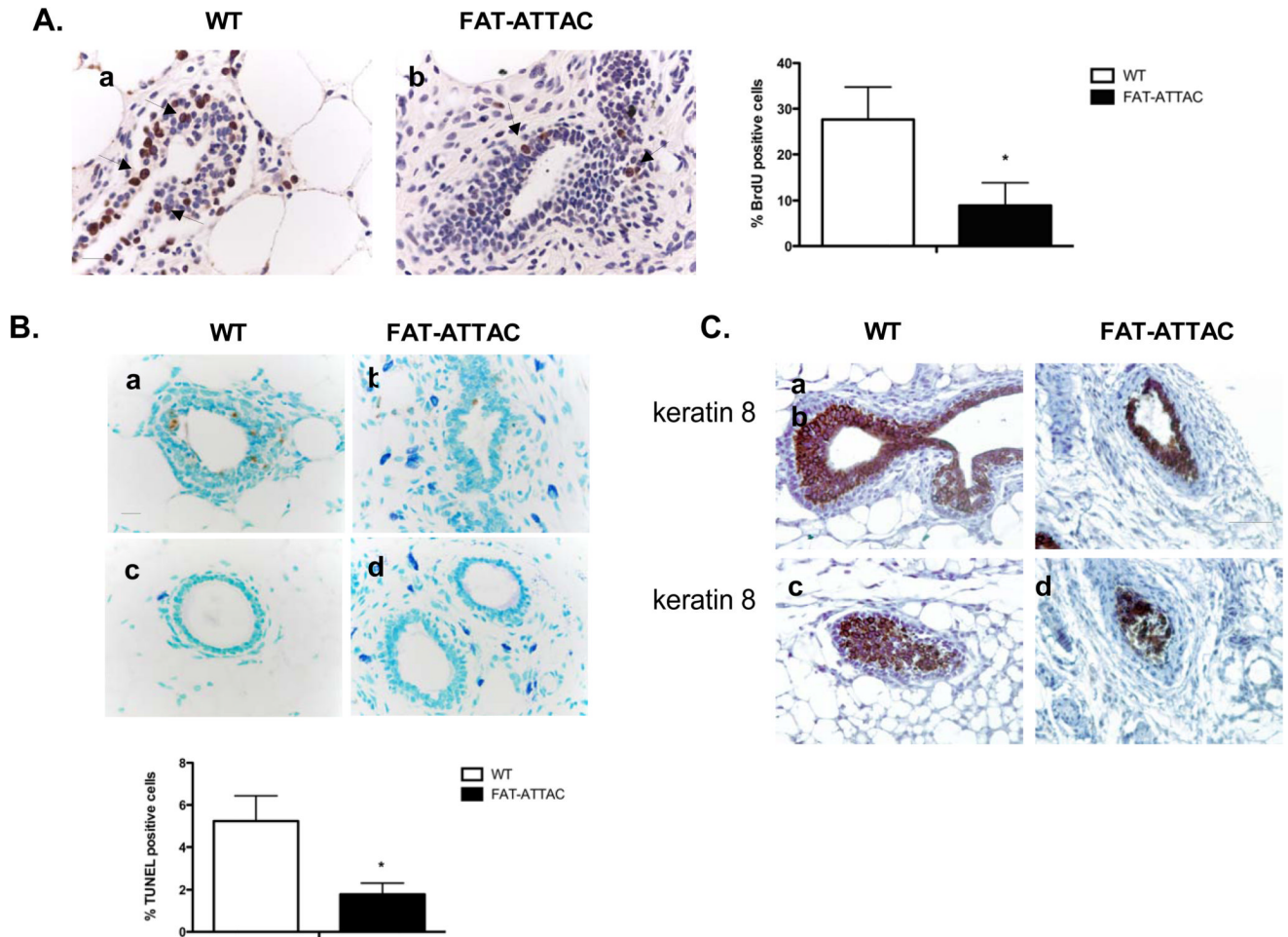


**Figure 6. Ablation of mammary stromal adipocytes results in inhibition of both proliferation and apoptosis**

**A)** BrdU immunohistochemistry was carried out on mammary glands derived from mice that were treated with the dimerizer for a 2-week period. Shown is the % BrdU positive cells per TEB field. (\* $p < 0.05$ ,  $n = 4$ /per group, Scale bar 20mm). **B)** TUNEL immunohistochemistry of mice dimerized for 4 weeks. Shown is quantification of the TUNEL immunohistochemistry per TEB field (\* $p < 0.05$ ,  $n = 4$ /per group, Scale bar 20mm). **C)** Mice were dimerized for 4 weeks and immunohistochemical analysis of TEBS was conducted using the luminal epithelial marker cytokeratin 8 ( $n = 5$ /per group, Scale bar 50mm).

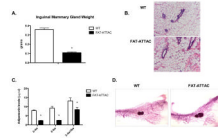


**Figure 7. Normalization of mammary gland growth following cessation of dimerizer treatment**

Mice were treated from 2-weeks of age for a period of 2 weeks followed by period of 2-weeks which injections of the dimerizer was ceased. At 6-weeks of age mice were sacrificed. **A)** Excised mammary gland were weighed, the mammary fat pad of FAT-ATTAC mice had a significantly smaller mass compared to wildtype mice ( $*p < 0.05$ ,  $n = 4$ /per group). **B)** H&E of FAT-ATTAC mammary glands demonstrate extensive patches of emerging adipose tissue regeneration, with the mammary ducts gradually adopting a normal morphology. **C)** Circulating adiponectin levels sharply decrease during dimerizer treatment by 70–75% as compared to wildtype mice. Cessation of the dimerizer treatment partially restores adiponectin levels to approximately 60% of wildtype levels (right hand bar). ( $*p < 0.05$ ). **D)** Whole-mount analysis demonstrated that the number of TEBs, and ductal extension although slightly lower in the transgenic mice, does not amount to a significant difference when compared to wildtype littermates. In contrast, the number of secondary branches are still significantly lower in FAT-ATTAC mammary glands compared to the wildtype littermates ( $n = 4$ /per group).

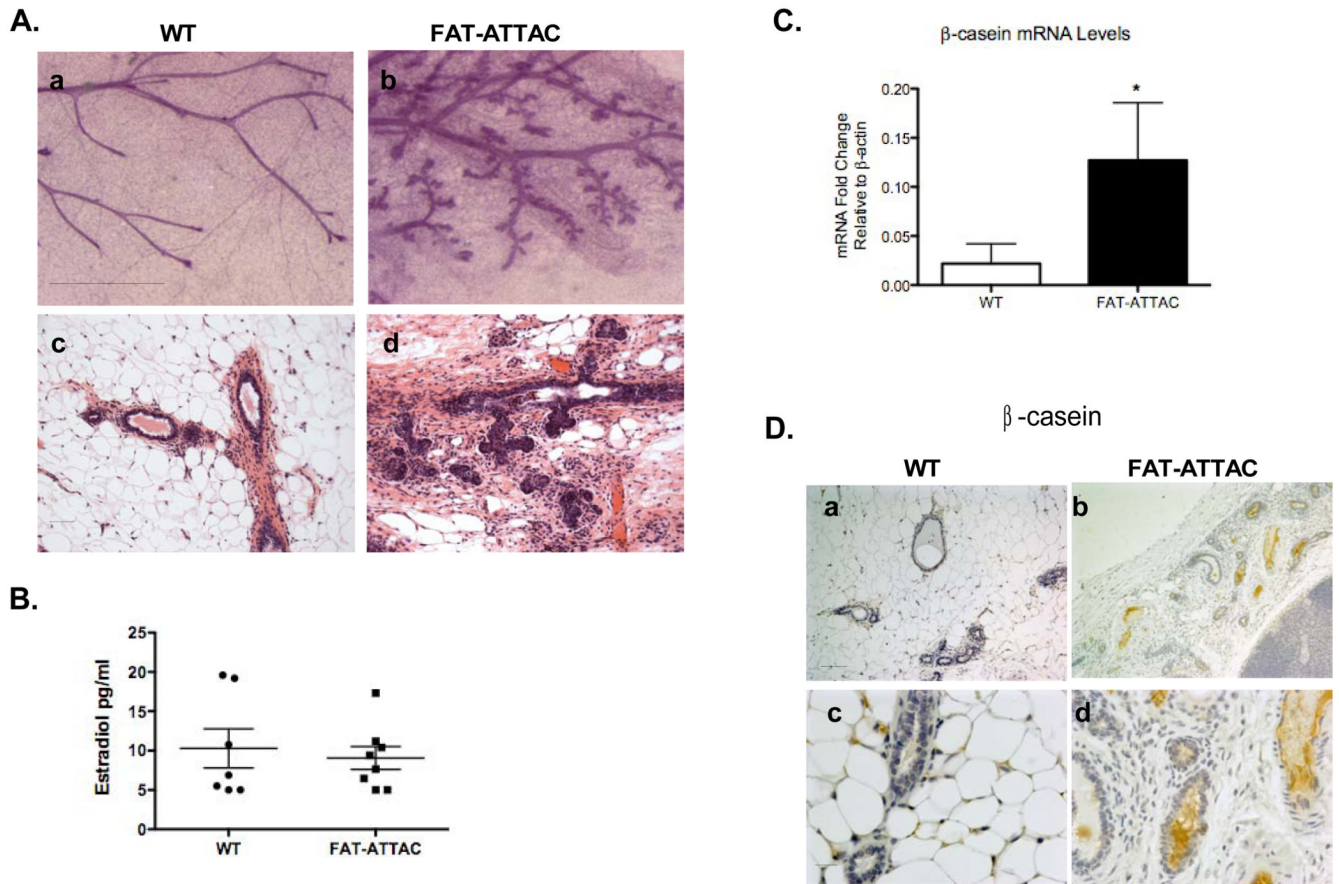


**Figure 8. Treatment of FAT-ATTAC mice during adulthood results in lobuloalveolar differentiation**

Mice were treated from 7-weeks of age for a period of 3 weeks. **A)** Whole-mounts and H&E are shown in panel a–b and panel c–e respectively. (Scale bar panel (a–b) 1mm, panel (c–d) 50mm, n=7–10/per group). Wild-type females are devoid of lobular-alveoli development, in contrast to FAT-ATTAC females, that display lobular-alveolar structures. **B)** Estradiol measurements determined in treated wild-type and FAT-ATTAC mice (n=7–8/per group). **C)** mRNA levels of b-casein. Total RNA was isolated from treated wild-type and FAT-ATTAC mammary glands (\*p<0.05, n=3–4/per group). **D)** Immunohistochemistry analysis was carried for b-casein in mammary glands (Scale bar panel (a–b) 100mm, panel (c–d) 20mm, n=5/per group).

**Table 1**  
**Normalization of mammary growth following cessation of dimerizer treatment**

Mice were treated from 2-weeks of age for a period of 2 weeks followed by period of 2-weeks which injections of the dimerizer was ceased. At 6-weeks of age mice were sacrificed. Data extracted from whole mounts analysis.

	WT	±SEM	FAT-ATTAC	±SEM	P-Value
# TEBs	11	1.08	8.7	3.2	NS
Average # of 2ry Branches	22.5	2.02	14.5	0.35	0.03
Ductal Extension in mm	8.3	0.68	9.9	0.58	NS